International Communications in Heat and Mass Transfer 125 (2021) 105316

Contents lists available at ScienceDirect

International Communications in Heat and Mass Transfer

journal homepage: www.elsevier.com/locate/ichmt

Buoyancy-driven flows beyond the Boussinesq approximation: A brief review

Peyman Mayeli *, Gregory J. Sheard

Department of Mechanical and Aerospace Engineering, Monash University, VIC 3800, Australia

ARTICLE INFO

Keywords:
Non-Boussinesq approximation
Non-Oberbeck—Boussinesq approximation
Buoyancy-driven flows
Free convection
Compressible natural convection

ABSTRACT

The well-known Boussinesq (also known as Oberbeck—Boussinesq) approximation is still the most common approach for the numerical simulation of natural convection problems. However, the accurate performance of this approximation is mainly restricted by small temperature differences. This encourages researchers and engineers to use other approaches beyond the range of validity of the Boussinesq approximation, especially when buoyancy-driven flows are generated by large temperature differences. This paper assembles and classifies the various approaches for numerical simulation of laminar natural convection, including Boussinesq and non-Boussinesq approximations for Newtonian fluids. These classifications reside under two overarching classes capturing compressible and incompressible approaches, respectively. This review elaborates on the different approaches and formulations adopted within each category.

1. Introduction

Natural convection (NC) describes the flow and associated heat transport generated by temperature or species molar concentration differences. The addition of an external momentum source (a fan, for example) creates the sister class of convection known as mixed convection. This paper focuses solely on pure natural convection problems in the absence of external momentum forcing and the different possible scenarios for their numerical simulation.

The name most synonymous with modelling natural convection is Joseph Valentin Boussinesq, who in 1897 proposed the striking simplification of the natural convection problem that now bears his name: the Boussinesq model [1] neglects density differences except in the gravity term of the momentum equation. Crucially, this permitted NC flows to be treated within an incompressible framework, greatly increasing their mathematical tractability. Almost fifty years after Claude Navier (in 1850) and George Stokes (in 1845) contributed to the development of the Navier—Stokes (NS) equations governing fluid motion, Boussinesq [1] established his famous approximation for NC problems. Later, Josef [2] recognised that Anton Oberbeck in 1879 [3] had earlier applied the same concept in his description of heat conduction in liquids accounting for currents driven by thermal gradients. The model is now commonly referred to as the Oberbeck—Boussinesq (OB) approximation in recognition of their respective contributions. The OB approximation is established based on the following assumptions:

- Small temperature differences
- Negligible viscous heat dissipation
- Constant thermophysical properties
- Linear density state equation
- Small hydrostatic pressure variations

Under the OB approximation, density variations are confined just to the gravity term of the momentum equation, and their effects are ignored in other terms. Simple implementation, rapid convergence rate, and outstanding accuracy over small temperature differences are benefits of the OB approximation. Under the OB approximation, density and temperature are connected via a linear density state equation using the definition of volumetric thermal expansion. The expansion coefficient value is typically taken at some reference temperature of the working fluid. Another less appreciated fundamental assumption of the OB approximation, is small hydrostatic pressure variations over the height of the physical domain compared to the thermodynamic pressure variations inside the system. This ratio is characterized by the dimensionless barometric number ($Ba = gH/RT$) [4].

One of the pioneering studies to determine the accurate range of the OB approximation performance was performed by Gray & Giorgini [5]. Considering all fluid properties as linear functions of two state variables (temperature and pressure) at a reference temperature of $T_0 = 15\ ^\circ C$ and

* Corresponding author.
E-mail addresses: peyman.mayeli@monash.edu (P. Mayeli), Greg.Sheard@monash.edu (G.J. Sheard).

https://doi.org/10.1016/j.icheatmasstransfer.2021.105316

Nomenclature

Ba	barometric number
c_p	specific heat at constant pressure
e_g	the unit vector in the gravity direction
Ec	Eckert number
Fr	Froude number
Ga	Gay-Lussac parameter ($\beta\Delta\theta$)
H	height
k	thermal conductivity
L	reference length
p	pressure
P	dimensionless pressure
Pth	thermodynamic pressure
Pr	Prandtl number
R	ideal gas constant
Ra	Rayleigh number
T	temperature
u	velocity vector
U	dimensionless velocity vector
α	thermal diffusivity
β	isobaric expansion coefficient
ε	relative temperature difference
θ	physical temperature
Θ	dimensionless temperature
μ	dynamic viscosity
ν	kinematic viscosity
ρ	density

a reference pressure of $p_0 = 1$ atm, they extracted the valid temperature difference range of the OB approximation application in air and water as respectively less than 28.6 ° C and 1.25 ° C at a limited length scale of $L_{ref} \leq 8.3 \times 10^4$ cm and $L_{ref} \leq 2.4 \times 10^5$ cm. To neglect the pressure work term in the energy equation, they obtained the ranges of $\Delta T/L_{ref} \leq 1020$ cm/ ° C and $\Delta T/L_{ref} \leq 9.9 \times 10^4$ cm/ ° C for air and water, respectively. Additionally, to safely ignore the viscous dissipation relative to the thermal diffusion term of the energy equation, they obtained length scales $L_{ref} \leq 4.1 \times 10^5$ cm and $L_{ref} \leq 3.5 \times 10^6$ cm for air and water, respectively.

There are many scientific and industrial applications in which temperature differences and length scales are beyond the regime of validity of the OB approximation. Foundry processes, thermal insulation systems in nuclear reactors, solar collectors, and astrophysical MHD simulations are some examples in which temperature differences are of the order of several hundred kelvin, or in which the length scale exceeds hundred kilometres. In these situations, the OB approximation yields inaccurate results. Available numerical algorithms that attempt to improve upon the OB approximation are less abundant in the literature. This paper seeks to classify numerical algorithms within two main categories: compressible and incompressible. These two categories and their sub-categories are presented in the context of a flowchart in Fig. 1. In section 2, compressible-flow approaches are introduced, and in section 3, incompressible approaches are reviewed. A brief conclusion is drawn in section 4. An exhaustive collation of the literature review pertaining to each of the identified sub-categories is beyond the scope of this review.

2. Compressible-flow based approximations

The first category of remedies to the limitations of the OB approximation is built upon the concept of compressibility, which leads to the introduction of the Mach number. As shown in Fig. 1, compressible treatment of the NS equations is possible in two fashions: Fully compressible and weakly compressible approaches. We start with the introduction of the fully compressible approach and numerical problems associated with that. Then, the weakly compressible approach is introduced and discussed.

2.1. Fully compressible approximation

Theoretically, the perfect simulation of NC is possible via the fully compressible form of the NS equations, since minimal approximations are introduced in this approach. The governing equations for a compressible Newtonian fluid, respectively derived from the principles of conservation of mass, momentum and energy, and closed by a density state equation are,

$$\begin{cases} \dfrac{\partial \rho^*}{\partial t^*} + \nabla \cdot (\rho^* \boldsymbol{u}) = 0, \\ \dfrac{\partial (\rho^* \boldsymbol{u})}{\partial t^*} + \nabla \cdot (\rho^* \boldsymbol{u} \otimes \boldsymbol{u}) = -\nabla p + \rho^* g \boldsymbol{e}_g + \mu \nabla \cdot \boldsymbol{\tau}^*, \\ \dfrac{\partial (\rho^* {c_p}^* T)}{\partial t^*} + \nabla \cdot \left(\rho^* {c_p}^* \boldsymbol{u} T\right) = k \nabla^2 T + \dfrac{\mathrm{D}p}{\mathrm{D}t^*} + \mu \varphi \\ p = f(\rho^*, T) \end{cases}, \tag{1}$$

It should be noted the energy equation does not have a unique form. Different forms of the energy equation including specific heat at constant volume (c_v) or shear stress ($\boldsymbol{\tau}$) may be found in ref. [6]. Using dimensionless parameters based on diffusion velocity scale ($u_0 = \alpha/L$),

$$t = \frac{t^* \alpha}{L^2}, \boldsymbol{X} = \frac{\boldsymbol{x}}{L}, \boldsymbol{U} = \frac{\boldsymbol{u} L}{\alpha}, P = \frac{p L^2}{\rho_0 \alpha^2}, \Theta = \frac{T}{T_0}, \rho = \frac{\rho^*}{\rho_0}, c_p = \frac{{c_p}^*}{c_{p0}}, \varepsilon = \frac{\Delta T}{2T_0}, \tag{2}$$

the dimensionless form of the fully compressible NS equations may be

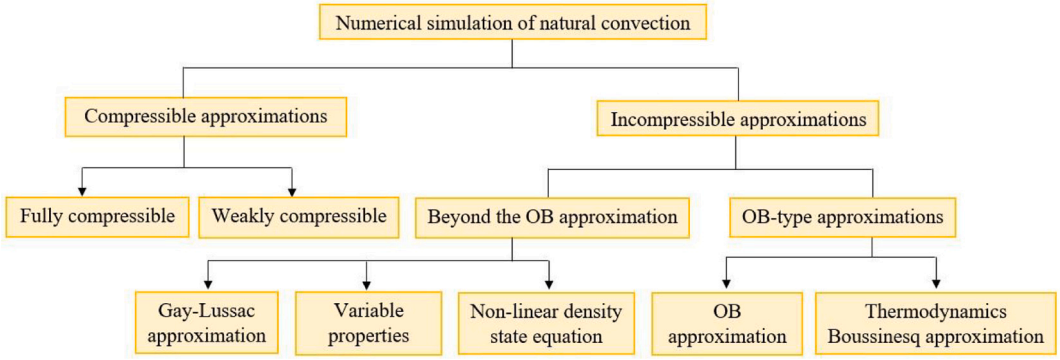

Fig. 1. Classification of different approximations for numerical simulation of the natural convection problems.

expressed as follows,

$$\begin{cases} \dfrac{\partial \rho}{\partial t} + \nabla \cdot (\rho \boldsymbol{U}) = 0, \\ \dfrac{\partial (\rho \boldsymbol{U})}{\partial t} + \nabla \cdot (\rho \boldsymbol{U} \otimes \boldsymbol{U}) = -\nabla P + \dfrac{RaPr}{2\varepsilon} \rho \boldsymbol{e}_g + Pr \nabla \cdot \boldsymbol{\tau}, \\ \dfrac{\partial (\rho \Theta)}{\partial t} + \nabla \cdot (\rho \boldsymbol{U} \Theta) = \nabla^2 \Theta + 2\varepsilon Ec \dfrac{\mathrm{D}P}{\mathrm{D}t} + 2\varepsilon Ec Pr \Phi \\ P = f(\rho, \Theta) \end{cases} \tag{3}$$

The choice for the reference velocity in NC is not unique. Another common choice for the reference velocity is the gravity velocity scale ($u_0 = \sqrt{g\beta\Delta TL}$), leading to different pre-factors. The presented dimensionless equation of state is also valid for an ideal diatomic gas ($R/R_0 = 1$, $c_p = 1$). Using Stokes' hypothesis for the bulk viscosity ($\lambda = -2/3\mu$), the dimensionless form of the stress tensor ($\boldsymbol{\tau}$) and dissipation term (Φ) for a 2D flow field in Cartesian coordinates are,

$$\boldsymbol{\tau} = \nabla \boldsymbol{U} + (\nabla \boldsymbol{U})^T - (2/3)(\nabla \cdot \boldsymbol{U}) \boldsymbol{I}, \tag{4}$$

$$\Phi = 2\left[\left(\frac{\partial U}{\partial X}\right)^2 + \left(\frac{\partial V}{\partial Y}\right)^2\right] + \left(\frac{\partial U}{\partial Y} + \frac{\partial V}{\partial X}\right)^2 - \frac{2}{3}\left[\left(\frac{\partial U}{\partial X} + \frac{\partial V}{\partial Y}\right)^2\right] \tag{5}$$

Compressible flow is characterized by the Mach number. In compressible buoyancy-driven flows, the square of the Mach number for an ideal gas may be recast as,

$$Ma^2 = \frac{{u_0}^2}{\gamma (\partial p/\partial \rho)_T} = \frac{(\alpha/L)^2}{\gamma R T_0} = \frac{(\alpha/L)^2}{(\gamma - 1) c p_0 T_0} = \frac{2\varepsilon}{(\gamma - 1)} \frac{(\alpha/L)^2}{c p_0 \Delta T} = \frac{2\varepsilon}{(\gamma - 1)} Ec. \tag{6}$$

Regarding the maximum value of the relative temperature difference of unity ($\varepsilon_{max} = 1$), the maximum Mach number in NC is bounded by the square root of the Eckert number ($Ma_{max} = \sqrt{2Ec(\gamma - 1)^{-1}}$). Another advantage of Eq. (6) is replacement of the $2\varepsilon Ec$ in the energy equation by $(\gamma - 1)Ma^2$. Thus, the energy equation may be rewritten as,

$$\frac{\partial (\rho \Theta)}{\partial t} + \nabla \cdot (\rho \boldsymbol{U} \Theta) = \nabla^2 \Theta + (\gamma - 1) Ma^2 \left(\frac{\mathrm{D}P}{\mathrm{D}t} + Pr \Phi\right) \tag{7}$$

When expressed in this form, it can be seen that the energy equation under the incompressible assumption is recovered as the Mach number approaches zero ($Ma \to 0, \rho \to 1$).

Fully compressible NS solvers are developed in two fashions: pressure-based and density-based. In brief, density-based algorithms are developed so that density is updated through the continuity equation, and pressure is obtained from the equation of state. The Roe scheme [7] is a popular method in this category. On the other hand, in pressure-based algorithms, the continuity equation becomes a constraint (Poisson equation) for pressure, and density is updated via the equation of state. While pressure-based algorithms can be applied across the entire spectrum of the Mach number, density-based solvers face serious convergence problems within the near-zero Mach number regime [8], as pressure wave speed approaches infinity as $Ma \to 0$. This is important because Mach number is typically very small for most NC problems. For instance, numerical simulation of NC in the square cavity benchmark problem (with two horizontal adiabatic sides and two vertical hot and cold isothermal walls) at a high relative temperature difference of $\varepsilon = 0.6$ and $Ra = 10^5$ indicates the maximum Mach number is equal to 3.68×10^{-4} [9]. Thus, applying density-based solvers on NC problems requires numerical treatments such as preconditioning and using a dual time-step strategy [10,11]. Although pressure-based algorithms would appear to be more suitable for NC problems, but for enclosed domains (having no inflow-outflow), conserving initial mass should be considered for a physical answer [12].

Many researchers have performed numerical simulations of NC problems under the fully compressible approach. NC in square cavity benchmark problem up to $Ra = 10^6$ and $\varepsilon = 0.6$ is numerically simulated in refs. [12–16]. Reported data corresponding to $\varepsilon = 0.01$ in refs. [12, 15, 16] confirm that the fully compressible approach gives identical results to the incompressible OB approximation. El-Gendi & Aly [17] analysed unsteady compressible NC in square and sinusoidal cavity up to a huge temperature difference of 2000 K. Darbandi and Hosseinizadeh [18] studied NC in a deep vertical-cavity, concluding that the maximum Nusselt number initially increases and then decreases as the length to height ratio increases with a little different pattern for different Rayleigh numbers. NC in a horizontal concentric annulus cavity at $Ra = 4.7 \times 10^4$ and $\varepsilon = 0.33$ under the fully compressible assumption is performed by Weiss and Smith [11]. A similar study within the OB regime ($\Delta T = 26.3\ ^\circ C$) was performed by Volkov *et al.* [19]. The aspect ratio of the outer to inner cylinder diameters in both studies was fixed at 2.6 to enable comparison with the experimental data reported by Kuhen & Goldstein [20]. Yamamoto *et al.* [21] simulated compressible NC of air around a circular cylinder in free space as an external flow and validated their results against the experimental data of Kuhen & Goldstein [20]. Then, they extended their calculations for NC of horizontal pipes containing hot liquid with three different solid to air conductivity ratio. Fu *et al.* [22] simulated a compressible NC problem in a vertical open channel for industrial applications. In this respect, they presented two equations, which separately correlates the average Nusselt number to the Rayleigh number and the length of the channel for a broad range of temperature differences. A similar study of compressible NC in an inclined open channel for a limited range of the Rayleigh number has been performed by Talukdar *et al.* [23]. Following Fu *et al.* [22], they presented a relation for the average Nusselt number as a function of Rayleigh number and inclination angle suitable for engineering applications.

2.2. Weakly compressible approximation

The second subcategory under the umbrella of compressible flow assumption, i.e. weakly compressible approach, is developed to resolve numerical problems associated with small Mach number NC problems. This approach is also sometimes called as the low Mach number scheme (LMS). Another advantage of the LMS approximation is that it permits larger time steps for explicit methods. Under the LMS approximation developed by Paulucci [24], acoustic sound waves are filtered from the fully compressible approach for the low Mach number regime, and the total pressure is split into a global/uniform thermodynamic pressure (p_{th}) and a local hydrodynamic pressure (p_h) as $p_{tot} = p_{th} + p_h$. This simplification is performed based on asymptotic analysis that states $p_{th}/p_0 \cong O(1)$ and $p_h/p_0 \cong O(Ma^2)$ [24]. Under the LMS approximation, local hydrodynamic pressure (obtained from a Poisson equation) acts in the momentum equation to establish a balance amongst advection, buoyancy, and diffusion terms, while thermodynamic pressure is used to update density during the solution procedure. Under the LMS approximation, the governing equations for an ideal gas are expressed as,

$$\begin{cases} \dfrac{\partial \rho^*}{\partial t^*} + \nabla \cdot (\rho^* \boldsymbol{u}) = 0, \\ \dfrac{\partial (\rho^* \boldsymbol{u})}{\partial t^*} + \nabla \cdot (\rho^* \boldsymbol{u} \otimes \boldsymbol{u}) = -\nabla p_h + \rho^* \boldsymbol{e}_g + \nabla \cdot \boldsymbol{\tau}^*, \\ \rho^* {c_p}^* \left(\dfrac{\partial T}{\partial t^*} + \boldsymbol{u} \cdot \nabla T\right) = \kappa \nabla^2 T + \dfrac{\mathrm{d}p_{th}}{\mathrm{d}t}, \\ p_{\mathrm{th}} = \rho^* R T. \end{cases} \tag{8}$$

Using the group of dimensionless parameters introduced earlier in Eq. (6) accompanied by a dimensionless thermodynamic pressure ($P_{th} = p_{th}/p_0$), the dimensionless form of the governing equations for an ideal gas are expressed as follows [25].

$$\begin{cases} \dfrac{\partial \rho}{\partial t} + \nabla \cdot (\rho \boldsymbol{U}) = 0, \\ \dfrac{\partial (\rho \boldsymbol{U})}{\partial t} + \nabla \cdot (\rho \boldsymbol{U} \otimes \boldsymbol{U}) = -\nabla P + \dfrac{RaPr}{2\varepsilon} \rho \boldsymbol{e}_g + Pr \nabla \cdot \boldsymbol{\tau}, \\ \rho \left(\dfrac{\partial \Theta}{\partial t} + \boldsymbol{U} \cdot \nabla \Theta \right) = \nabla^2 \Theta + \Gamma \dfrac{\mathrm{d}P_{th}}{\mathrm{d}t}, \\ P_{th} = \rho \Theta. \end{cases} \tag{9}$$

In Eq. (9), Γ is a measure of the resilience of the fluid ($\Gamma = (\gamma - 1)/\gamma$), where γ is the heat capacity ratio ($\gamma = c_p/c_v$). The buoyancy term in both of Eqs. (3) and (9) is expressed by a gL^3/α^2 pre-factor that is replaced by a Froude number, characterising the ratio of inertia to gravity,

$$\frac{gL^3}{\alpha^2}\rho = \frac{gL}{(\alpha/L)^2}\rho = \frac{gL}{{u_0}^2}\rho = \frac{1}{Fr}\rho. \tag{10}$$

To express the Froude number as a Product of Ra, Pr, and ε, we may use the Rayleigh number definition. Within the compressible/weakly-compressible approaches, the Rayleigh number is expressed slightly differently compared to its incompressible definition

$$Ra_{comp.} = Pr\frac{g{\rho_0}^2(T_h - T_c)L^3}{T_o{\mu_0}^2} = \frac{g\beta\Delta TL^3}{\nu\alpha} = Ra_{incomp.} \tag{11}$$

Comparing incompressible and compressible Rayleigh number definitions give the following relation for the Froude number,

$$\underbrace{2\varepsilon = (T_h - T_c)/T_o}_{\text{Compressible}} = \underbrace{\beta\Delta T = RaPrFr}_{\text{Incompressible}} \rightarrow Fr = 2\varepsilon \Big/ RaPr. \tag{12}$$

Eq. (9) has one more unknown (P_{th}) concerning the number of equations. For open systems, thermodynamic pressure may be simply approximated by the atmospheric pressure. However, for the enclosed domains, an extra equation is required to close the system of equations. Combining the energy equation with the equation of state and continuity from Eq. (9) yields,

$$\nabla \cdot \boldsymbol{U} = \frac{1}{p_{th}} \left[\nabla^2 \Theta - \frac{1}{\gamma} \frac{\mathrm{d}P_{th}}{\mathrm{d}t} \right] \tag{13}$$

Using the Gauss divergence theorem, it can be shown that integration of $\nabla \cdot \boldsymbol{U}$ over a closed domain is zero, thus

$$\frac{\mathrm{d}P_{th}}{\mathrm{d}t} = \frac{\gamma}{V} \int_S \frac{\partial \Theta}{\partial x_j} n_j \mathrm{d}S. \tag{14}$$

In Eq. (14), S and V refer to the surface and volume of the physical domain, respectively. The integrand of Eq. (14) is the residual of the energy equation that asymptotically goes to zero for a steady-state solution ($\mathrm{d}P_{th}/\mathrm{d}t \rightarrow 0$). Computing thermodynamic pressure variations from Eq. (14) does not guarantee strict mass conservation [9]. Knowing initial mass inside the system (m_0), Le Quéré et al. [26] suggested applying the concept of mass conservation for an enclosed domain to update thermodynamic pressure:

$$m_0 = \frac{P_0 V}{RT_0} = \frac{P_{th} V}{RT} \rightarrow P_{th} = \underbrace{\left(\frac{P_0 V}{T_0}\right)}_{cte} \Big/ \int_V \mathrm{d}V \Big/ T. \tag{15}$$

A comprehensive study of the NC under the LMS approximation in the square cavity benchmark problem is performed by Paolucci and Chenoweth [25,27]. They found that by increasing temperature differences, critical Ra for stationary and oscillatory instabilities are decreased. Their stability analysis results under LMS approximation for a differential relative temperature difference indicates that flow becomes unsteady at $Ra = 1.93 \times 10^8$ [27]. A similar study of the NC problem under the LMS approximation in the square cavity is also performed by Wang et al. [28]. They extracted power-law scaling of the average Nusselt number for the different range of Ra at different ε and determined critical Rayleigh number at $\varepsilon = 0.2$, 0.4, and 0.6. A benchmark solution for the square cavity problem is provided by Le Quéré *et al.* [29]. Le Quéré *et al.* [26] applied LMS approximation for different relative temperature differences in a deep cavity with an aspect ratio of 8 to study the transition to unsteadiness. A similar study of a deep vertical-cavity emphasizing stability analysis is also performed by Suslov and Paolucci [30,31]. Paillere *et al.* [9] compared results of the LMS approach against the fully compressible approach for both small ($\varepsilon = 0.01$) and large ($\varepsilon = 0.6$) temperature differences up to $Ra = 10^5$. They showed the LMS model could simulate NC with high fidelity and negligible differences compared to the hyperbolic fully compressible NS equations. Elmo & Cioni [32] used LMS approximation for a pebble bed of a nuclear reactor. Kumar & Natarajan [33] investigated the role of discrete conservation in numerical simulations of thermos-buoyant flows in enclosures and devised two different pressure-based numerical algorithms under LMS approximation that violate either the equation of state or a conservation law at the discrete level, leading to two different classes of algorithms. Tyliszczak [34] applied the projection method with a second-order temporal accuracy of Adams-Bashforth/Adams-Moulton methods to the LMS approach.

Finally, in the compressible framework, the idea of splitting the total pressure into a spatially uniform and a local pressure is also presented under the homobaricity approach [35]. This approach was originally developed for gaseous flow with zero viscosity; similar to the LMS approach, equation of state and energy equations are treated by the spatially uniform thermodynamic pressure while the hydrodynamic local pressure acts solely in the momentum equation. Cherkasov *et al.* [36] applied this approach for a 1D boundary layer problem along the vertical plate.

3. Incompressible approximations

Approaches within the incompressible-flow framework will now be explored. As shown in Fig. 1, the incompressible category is divided into the OB type approximations and algorithms beyond the OB approximations. The OB-type approximations will be covered first, and then we introduce different non-OB subcategories will be discussed.

3.1. OB type approximations

The OB-type approximations may be divided into two groups; the first being the original OB approximation and the second being the thermodynamic Boussinesq approximation.

3.1.1. OB approximation

When the OB approach conditions [5] are met, density variations are assumed to be negligible except via the gravity term. Neglecting viscous heat dissipation and pressure work terms, governing equations in the dimensional form under the OB approximation are expressed as follows,

$$\begin{cases} \rho/\rho_0(\nabla \cdot \boldsymbol{u}) = 0 \\ \rho/\rho_0(\partial \boldsymbol{u}/\partial t^* + \boldsymbol{u} \cdot \nabla \boldsymbol{u}) = -(1/\rho_0)\nabla p + \nu \nabla^2 \boldsymbol{u} + (\rho/\rho_0) g \boldsymbol{e}_g \\ \rho/\rho_0(\partial T/\partial t^* + \boldsymbol{u} \cdot \nabla T) = \alpha \nabla^2 T. \end{cases} \tag{16}$$

To relate temperature variations to density, a linear density state equation ($\rho/\rho_0 = 1 - \beta\theta$) is derived from the volumetric thermal expansion coefficient definition. Under the OB approximation, all ρ/ρ_0 pre-factors are considered equal to unity except in gravity term, which is replaced by the linear density state equation. The result is,

$$\begin{cases} \nabla \cdot \boldsymbol{u} = 0 \\ \partial \boldsymbol{u}/\partial t^* + \boldsymbol{u} \cdot \nabla \boldsymbol{u} = -(1/\rho_0)\nabla p + \nu \nabla^2 \boldsymbol{u} + (1 - \beta\theta) g \boldsymbol{e}_g \\ \partial T/\partial t^* + \boldsymbol{u} \cdot \nabla T = \alpha \nabla^2 T. \end{cases} \tag{17}$$

In the next step, a modified pressure is introduced as $p^* = p + \rho_0 \phi$, where ϕ is the gravitational potential whose gradient opposes the gravitational acceleration vector, i.e. $\nabla \phi = -g\boldsymbol{e}_g$. The modified pressure absorbs $g\boldsymbol{e}_g$ term in the momentum equation and just the $\beta\theta g\boldsymbol{e}_g$ remains

as the buoyancy term. Using the same dimensionless parameters in Eq. (2) except with a different dimensionless temperature defined as $\Theta = (T - T_0)/\Delta T$, the dimensionless form of the governing equations become,

$$\begin{cases} \nabla \cdot \boldsymbol{U} = 0, \\ \partial \boldsymbol{U}/\partial t + \boldsymbol{U} \cdot \nabla \boldsymbol{U} = -\nabla P + Pr \nabla^2 \boldsymbol{U} - RaPr\Theta \boldsymbol{e}_g, \\ \partial \Theta/\partial t + \boldsymbol{U} \cdot \nabla \Theta = \nabla^2 \Theta. \end{cases} \tag{18}$$

There are a vast number of works that have adopted the OB approximation. As the focus of this review is on the approaches beyond the original OB approximation, interested readers are directed to relevant review papers with a focus on specific geometry including the annulus [37,38], triangular [39,40], parallelogram [41], non-square [42], and rectangular-shaped [43] cavities or particular topics within NC such as localized heating [44] or internal heat sources [45].

3.1.2. Thermodynamic Boussinesq approximation

Under the OB approximation, dissipated heat due to viscous friction and work of pressure stress are removed from the energy equation as their effects are assumed to be negligible. Decisions as to whether heat dissipation or pressure work terms may be neglected are typically made based on comparing order-of-magnitude arguments, but this causes a thermodynamical paradox. The momentum equations compel the dissipation of kinetic energy due to fluid friction (diffusion terms). However, under the OB approximation, heat produced by this process is not captured by the energy equation. Separately, the absence of the pressure work in the energy equation lacks a logical relation between the internal energy and work performed upon the fluid. Using Gibbs and entropy balance equations, it can be shown that when these contributions are omitted from the energy equation, the described thermodynamic system recognizes heat conduction (and not viscous friction) as the only source of irreversibility. This prompted to development of an elaborated version of the OB approximation under different names including 'deep convection' [46], 'thermodynamic' [47], and 'extended' [5] Boussinesq approximations. The thermodynamic paradox is discussed in detail in refs. [48, 49], where it is concluded that removing pressure work and viscus dissipated heat remains a paradox for enclosed domains. Pons and Le Quéré [50] presented a dimensionless form of the governing equations under the thermodynamic Boussinesq model in which the effect of both dissipated heat due to viscous friction and work of pressure stress were considered in the energy equation. When both terms mentioned above are considered in the energy equation, the governing equations for an ideal gas are,

$$\begin{cases} \nabla \cdot \boldsymbol{U} = 0, \\ \partial \boldsymbol{U}/\partial t + \boldsymbol{U} \cdot \nabla \boldsymbol{U} = -\nabla P + Pr \nabla^2 \boldsymbol{U} - RaPr\Theta \boldsymbol{e}_g, \\ \partial \Theta/\partial t + \boldsymbol{U} \cdot \nabla \Theta = \nabla^2 \Theta + EcPr\Phi - Ar\Gamma Ba \boldsymbol{U} \cdot \boldsymbol{e}_g, \end{cases} \tag{19}$$

where Φ is the dissipation term (Eq. (5)) of a divergence-free flow field and the barometric number is defined by the ratio of potential energy variations to thermodynamic pressure variations ($Ba = gH/R\Delta T$). Ar is the aspect ratio of the geometry ($Ar = L/H$). Since the net product of $EcPr$ is minimal for gaseous flow in the Boussinesq regime, Pons and Le Quéré [51] ignored dissipated heat due to viscous friction. They found that when the magnitude of the barometric number becomes more extensive than $0.01/\Gamma$, its effect in the energy equation is no longer negligible in the square cavity benchmark problem. A variant of the thermodynamic Boussinesq approximation whereby the pressure work is neglected and only the viscous dissipation term is retained, is broadly used for numerical simulation of NC in porous media. An excellent review of free/mixed convection in saturated porous media considering viscous dissipation is performed by Nield [52].

3.2. Non-OB approximations

Approaches residing in the second category of the incompressible approximations attempt to increase the OB approximation accuracy so that the formulation is applicable for a larger spectrum of temperature differences. With reference to Fig. 1, three subcategories are identified in this class: the Gay-Lussac approximation, non-linear density state equation, and approaches based on variable thermophysical properties.

3.2.1. Gay-Lussac approximation

Under the Gay-Lussac approximation, density variations are not confined only to gravity term in contrast to the OB approximation. In this approach, the ρ/ρ_0 pre-factors are expressed in terms of Gay-Lussac parameter ($Ga = \beta\Delta\theta$) as follows,

$$\rho/\rho_0 = 1 - \beta\theta = 1 - \beta\Delta\theta\Theta = 1 - Ga\Theta. \tag{20}$$

Considering all density variations of Eq. (16) and replacing them with Eq. (20) yields the following dimensionless form of the governing equations, which is known as the Gay-Lussac approximation,

$$\begin{cases} (1 - Ga\Theta)(\nabla \cdot \boldsymbol{U}) = 0 \\ \partial \boldsymbol{U}/\partial t + (1 - Ga\Theta)\boldsymbol{U} \cdot \nabla \boldsymbol{U} = -\nabla P + Pr \nabla^2 \boldsymbol{U} - RaPr\Theta \boldsymbol{e}_g \\ \partial \Theta/\partial t + (1 - Ga\Theta)\boldsymbol{U} \cdot \nabla \Theta = \nabla^2 \Theta. \end{cases} \tag{21}$$

Eq. (21) is made dimensionless with the same dimensionless parameters applied for the OB approximation. Having a physical density requires $\rho/\rho_0 > 0$ and consequently $1 - Ga\Theta > 0$ that gives $Ga < 1/\Theta$. When the dimensionless temperature is defined as $\Theta = (T - T_0)/\Delta T$, then the minimum and maximum dimensionless temperatures alter between ± 0.5 that gives $Ga < 2$ constraint for the Gay-Lussac parameter to have a physical density value. This approximation has thus far found only limited application in the literature. Pesso & Piva [53] applied the Gay-Lussac approximation for the square cavity benchmark problem for a broad range of Rayleigh ($10 \leq Ra \leq 10^8$) and Prandtl number ($0.0071 \leq Pr \leq 7.1$). Their calculations indicate a reverse relation between Ga and the average Nusselt number. They also presented an analytical relation predicting the average Nusselt number as a function of Ra, Pr, and Ga. Lopez *et al.* [54] presented a Gay-Lussac type approach for the treatment of rapidly rotating flows, in which instead of considering density variations in any term of the governing equations including density, buoyancy effects were extended just to the centrifugal part of the advection term to capture centrifugal effects in rapidly rotating flows. Mayeli & Sheard [55,56] continued this approach for NC in the annulus cavity with large temperature differences up to $\varepsilon = 0.2$. They compared obtained results against the LMS and OB approximations, concluding that extending density variations to the advection term slightly improves the Gay-Lussac type approximation flow-related data.

3.2.2. Non-linear density state equation

The full density state equation is $\rho/\rho_0 = 1 + \sum_{i=1}^{n}(-\beta\theta)^i$, that is derived from the volumetric thermal expansion coefficient definition. The OB approximation is established based on a linear density state equation ($n = 1$), which works very well for the small temperature differences. However, as the temperature differences become large, higher terms of the density state relation may no longer be negligible. Another justification for applying a non-linear density state relation comes from the unconventional behaviour of some fluids such as water at temperatures close to or equal to the temperature of maximum density (T_{max}). In this situation, the linear density state relation may not be valid, even for small temperature differences. For instance, the density-temperature relationship of cold water in the vicinity of 4 °C does not obey a linear function. The non-linear density state equation of water ($\rho/\rho_{max} = 1 - \beta\theta^q$ where $\beta = 9.29 \times 10^{-6}(^\circ\mathrm{C})^{-q}$ and $q = 1.894$) proposed by Gebhart and Mollendorf [57] is a popular equation in this category. Defining a dimensionless temperature named *inversion parameter* as $\Theta_m = (T_{max} - T_c)/(T_h - T_c)$ which relates the temperature of the maximum density to the hot and cold reference temperatures accompanied by a modified Rayleigh number defined as $Ra = g\beta\Delta T^q L^3/\nu\alpha$, the dimensionless momentum equation is expressed as follows in this category,

$$\partial \boldsymbol{U}/\partial t + \boldsymbol{U} \cdot \nabla \boldsymbol{U} = -\nabla P + Pr \nabla^2 \boldsymbol{U} - RaPr(\Theta - \Theta_m)^q \boldsymbol{e}_g. \tag{22}$$

For $0 < \Theta_m < 1$, T_{max} lies between the hot and cold reference temperatures. Thus, studies in this category focus on this regime and the corresponding flow patterns due to different inversion parameters. One of the pioneer studies in this category was performed by Nansteel *et al.* [58] in the small range of the Rayleigh number in a rectangular cavity with three different height to length aspect ratios. They found that the inversion parameter near 0.5 ($\Theta_m = 0.5$) results in a counter-rotating pair of vortices arranged horizontally in the enclosure. Similar behavior of dual rotating vortices in this problem is also reported by Braga & Viskanta [59]. Osorio *et al.* [60] studied this problem in an inclined square cavity. Another pioneering study in this category for the annulus cavity using a 4th-order density state equation is performed by Vasseur *et al.* [61]. They noticed a secondary vortex pair at the top of the inner cylinder for a limited range of inversion parameters. Raghavarao & Sanyasiraju [62] repeated this problem with a second-order density equation of state. They noticed a uni-cellular flow pattern at $\Theta_m = 0$ and 1, and a bi- cellular flow pattern at $\Theta_m = 0.5$. Ho & Lin [63] studied the NC of water close to its maximum density in eccentric annulus using Gebhart and Mollendorf equation of state [57]. Studying the NC of water around the horizontal cylinder in free space using a 4th-order density state equation is performed by Wang *et al.* [64]. In this category, the quadratic density state equation is also used for numerical simulation of the oscillatory NC in the square cavity [65].

3.2.3. *Variable thermophysical properties*

In the OB regime limit, the thermophysical properties of the working fluid are considered constant, which is a valid assumption for small temperature differences. However, when the temperature differences become large enough, the constant properties assumption is no longer valid, especially for working fluids sensitive to the temperature differences. Since most of the compressible/weakly compressible simulations are devoted to large temperature differences, the idea of applying variable thermophysical properties is applied by default to the formulation in those works [15–17,22–32]. This approach is also pursued in an incompressible category beyond the OB approximation. One of the pioneer studies in this category is performed by Zhong *et al.* [66]. Their numerical results of NC via variable thermophysical properties approach in the square cavity for air as working fluid confirms that up to $\varepsilon = 0.05$, the results of OB is valid. Also, at $\varepsilon \cong 0.1$, OB still correctly predicts overall heat transfer, but it over predicts the maximum vertical velocity by approximately 20%. Zhong *et al.* [66] also presented a relation for relative temperature difference as a function of the Rayleigh number determining the OB approximation's valid performance. Leal *et al.* [67] continued this approach and concluded that the properties variation effects are considerable even within the OB regime. Hernández & Zamora [68] applied this approach for vertical channels. Mahony *et al.* [69] studied the annulus cavity problem under variable thermophysical properties assumption. They found that the OB assumption over-predicts the tangential velocity and the temperature gradient near the hot inner cylinder while under-predicting both close to the cold outer cylinder. In this category, a similar study of the annulus cavity considering eccentric effects is also performed by Shahraki [70].

4. Conclusion

This review provides a general framework of different numerical approaches beyond the Oberbeck—Boussinesq approximation for buoyancy-driven flows. Two main approaches, compressible and incompressible, are distinguished, with different strategies elucidated within each class. A brief review of pioneering studies in each category is also performed. This short communication paper does not cover the broader literature on non-Oberbeck—Boussinesq natural convection, but the presented framework, in theory, may categorize any publication in this field of study. The literature survey indicates that, however the current compressible approaches work with high accuracy for natural convection problems associated with large temperature differences, but it seems the main challenge of the future non-Oberbeck—Boussinesq approximations would be improving the accuracy of the computations while retaining the simplicity of an incompressible approach.

Declaration of Competing Interest

None.

Acknowledgements

This research was supported by the Australian Research Council through Discovery Project DP180102647. P. M. is supported by a Monash Graduate Scholarship and a Monash International Postgraduate Research Scholarship.

References

[1] J. Boussinesq, Theorie Analytique de la Chaleur, Gauthier-Villars, Paris, 1897.
[2] D.D. Josef, Stability of Fluid Motions II, Springer, Berlin, 1976.
[3] A. Oberbeck, Ueber die Wärmeleitung der Flüssigkeiten bei Berücksichtigung der Strömungen infolge von Temperaturdifferenzen, Annual Rev Chem 7 (1879) 271.
[4] S. Lenz, M. Krafczyk, M. Geier, S. Chen, Z. Guo, Validation of a two-dimensional gas-kinetic scheme for compressible natural convection on structured and unstructured meshes, Int. J. Thermal Sci. 136 (2019) 299–315.
[5] D.D. Gray, A. Giorgini, The validity of the Boussinesq approximation for liquids and gases, Int. J. Heat Mass Transf. 19 (5) (1976) 545–551.
[6] J.D. Anderson, Computational fluid dynamics: the basics with applications, McGraw-Hill, 1995.
[7] P.L. Roe, Approximate Riemann solvers, parameter vectors, and different schemes, J. Comput. Phys. 43 (2) (1981) 357–372.
[8] K.C. Karki, S.V. Patankar, Pressure based calculation procedure for viscouse flows at all speeds in arbitrary configurations, AIAA J. 27 (9) (1989) 1167–1174.
[9] H. Paillere, C. Viozat, A. Kumbaro, I. Toumi, Comparison of low Mach number models for natural convection problems, Heat Mass Transf. 36 (2000) 567–573.
[10] E. Turkel, Review of preconditioning methods for fluid dynamics, Appl. Numer. Math. 12 (1–3) (1993) 257–284.
[11] J.M. Weiss, W.A. Smith, Preconditioning applied to variable and constant density flows, AIAA J. 33 (11) (1995) 2050–2057.
[12] S. Mazumder, On the use of the fully compressible Navier-Stokes equations for the steady-state solution of natural convection problems in closed cavities, ASME: *J. Heat Transf.* 129 (2007) 387–390.
[13] Y.H. Choi, C.L. Merkle, The Application of Preconditioning in Viscous Flows, J. Comput. Phys. 105 (2) (1993) 207–223.
[14] S.T. Yu, B.N. Jiang, J. Wu, N.S. Liu, A Div-Curl-Grad Formulation for compressible buoyant flows solved by the least-squares finite-element method, Comput. Methods Appl. Mech. Eng. 137 (1) (1996) 59–88.
[15] J. Vierendeels, B. Merci, E. Dick, Numerical study of natural convective heat transfer with large temperature differences, Int. J. Numer. Methods heat fluid flow 11 (4) (2001) 329–341.
[16] M. Drabandi, S.F. Hosseinizadeh, Numerical simulation of thermobuoyant flow with large temperature Variation, JTHT 20 (2) (2006).
[17] M.M. El-Gendi, A.M. Aly, Numerical simulation of natural convection using unsteady compressible Navier-stokes equations, Int. J. Numer. Methods heat fluid flow 27 (11) (2017) 2508–2527.
[18] M. Drabandi, S.F. Hosseinizadeh, Numerical Study of natural convection in vertical enclosures using a novel non-Boussinesq algorithm, Numer. Heat Transf. Part A 52 (9) (2007) 849–873.
[19] K.N. Volkov, V.N. Emel'yanov, A.G. Karpenko, Preconditioning of Navier–Stokes equations in the computation of free convective flows, Comput. Math. Math. Phys. 55 (2015) 2080–2093.
[20] T.H. Kuhen, R.J. Goldstein, An experimental and theoretical study of natural convection in the annulus between horizontal concentric cylinders, J. Fluid Mech. 74 (4) (1976) 695–719.
[21] S. Yamamoto, D. Niiyama, B.R. Shin, A numerical method for natural convection and heat conduction around and in a horizontal circular pipe, Int. J. Heat Mass Transf. 47 (26) (2004) 5781–5792.
[22] W.S. Fu, C.G. Li, C.P. Huang, J.C. Huang, An investigation of a high temperature difference natural convection in a finite length channel without Boussinesq assumption, Int. J. Heat Mass Transf. 52 (11–12) (2009) 2571–2580.
[23] D. Talukdar, C.G. Li, M. Tsubokura, Numerical investigation of laminar compressible natural convection flow in asymmetrically and isothermally heated open-ended inclined channel, Int. J. Heat Mass Transf. 130 (2019) 83–97.
[24] S. Paolucci, On the filtering of sound from the Navier-Stokes equations, Technical report 9, Sandia National Laboratories, 1982. SAND 82–8257.
[25] D.R. Chenoweth, S. Paolucci, Natural convection in an enclosed vertical air layer with large horizontal temperature differences, J. Fluid Mech. 169 (1986) 173–210.
[26] P. Le Quéré, R. Masson, P. Perrot, A Chebyshev collocation algorithm for 2D non-Boussinesq convection, J. Comput. Phys. 103 (2) (1992) 320–335.
[27] S. Paolucci, D.R. Chenoweth, Transition to chaos in a differentially heated vertical cavity, J. Fluid Mech. 201 (1989) 379–410.

[28] Q. Wang, S.N. Xia, R. Yan, D.J. Sun, Z.H. Wan, Non-Oberbeck-Boussinesq effects due to large temperature differences in a differentially heated square cavity filled with air, Int. J. Heat Mass Transf. 128 (2019) 479–491.
[29] P. Le Quéré, C. Weisman, H. Paillère, J. Vierendeels, E. Dick, R. Becker, M. Braack, J. Locke, Modelling of natural convection flows with large temperature differences: a benchmark problem for low Mach number solvers. Part 1. Reference solutions, Esaim Math Model Numer Anal **39** (3) (2005) 609–616.
[30] S.A. Suslov, S. Paolucci, Non-linear analysis of convection flow in a tall vertical enclosure under non-Boussinesq conditions, J. Fluid Mech. 344 (1997) 1–41.
[31] S.A. Suslov, S. Paolucci, Stability of natural convection flow in a tall vertical enclosure under non-Boussinesq condition, Int. J. Heat Mass Transf. 38 (12) (1995) 2143–2157.
[32] M. Elmo, O. Cioni, Low Mach number model for compressible flows and application to HTR, Nucl. Eng. Des. 222 (2–3) (2003) 117–124.
[33] M. Kumar, G. Natarajan, On the role of discrete mass conservation for non-Boussinesq flow simulations in enclosures, Int. J. Heat Mass Transf. 104 (2017) 1283–1299.
[34] A. Tyliszczak, Projection method for high-order compact schemes for low Mach number flows in enclosures, Int. J. Numer. Methods heat fluid flow 24 (5) (2014) 1141–1174.
[35] S.G. Cherkasov, Some special features of description of thermal and dynamic processes in gases in the approximation of homobaricity, High Temp. 48 (2010) 422–426.
[36] S.G. Cherkasov, A.V. Anan'ev, L.A. Moiseeva, Limitations of the Boussinesq model on the example of laminary natural convection of gas between vertical isothermal walls, High Temp. 56 (2018) 878–883.
[37] D. Angeli, G.S. Barozzi, M.W. Collins, O.M. Kamiyo, A critical review of buoyancy-induced flow transitions in horizontal annuli, Int. J. Therm. Sc. 49 (2010) 2231–2241.
[38] H.K. Dawood, H.A. Mohammedb, Nor Azwadi Che Sidik, K.M. Munisamy, M. A. Wahid, Forced, natural and mixed-convection heat transfer and fluid flow in annulus: A review, Int. Commun. Heat & Mass **62** (2015) 45–57.
[39] S.C. Saha, M.M.K. Khan, A review of natural convection and heat transfer in attic-shaped space, Energy Build 43 (2011) 2564–2571.
[40] O.M. Kamiyo, D. Angeli, G.S. Barozzi, M.W. Collins, V.O.S. Olunloyo, S.O. Talabi, A Comprehensive review of natural convection in triangular enclosures, ASME: Appl. Mech. Rev 63 (6) (2010), 060801–1:13.
[41] A. Baïri, E. Zarco-Pernia, J.M. García de María, A review on natural convection in enclosures for engineering applications, The particular case of the parallelogrammic diode cavity, Appl. Therm. Eng. 63 (2014) 304–322.
[42] D. Das, M. Roy, T. Basak, Studies on natural convection within enclosures of various (non-square) shapes – A review, Int. J. Heat Mass Transf. 106 (2017) 356–406.
[43] I.V. Miroshnichenko, M.A. Sheremet, Turbulent natural convection heat transfer in rectangular enclosures using experimental and numerical approaches: A review, Renew. Sust. Energ. Rev. 82 (2018) 40–59.
[44] H.F. Öztop, P. Estellé, W.M. Yan, K. Al-Salem, J. Orfi, O. Mahian, A brief review of natural convection in enclosures under localized heating with and without nanofluids, Int. Commun. Heat & Mass 60 (2015) 37–44.
[45] S. Pandey, Y.G. Park, M.Y. Ha, An exhaustive review of studies on natural convection in enclosures with and without internal bodies of various shapes, Int. J. Heat Mass Transf. 138 (2019) 762–795.
[46] E.A. Spiegel, G. Veronis, On the Boussinesq approximation for a compressible fluid, Astrophys. J. 131 (1960) 442.
[47] J.A. Dutton, G.H. Fichtl, Approximate equations of motion for gases and liquid, J. Atmos. Sci. 26 (2) (1969) 241–254.
[48] A. Barletta, Comments on a paradox of viscous dissipation and its relation to the Oberbeck–Boussinesq approach, Int. J. Heat Mass Transf. 51 (2008) 6312–6316.
[49] A. Barletta, Local energy balance, specific heats and the Oberbeck-Boussinesq approximation, Int. J. Heat Mass Transf. 52 (2009) 5266–5270.
[50] M. Pons, P. Le Quéré, An example of entropy balance in natural convection, Part 2: the thermodynamic Boussinesq equations, Comptes Rendus Mécanique 333 (2) (2005) 133–138.
[51] M. Pons, P. Le Quéré, Modeling natural convection with the work of pressure-forces: a thermodynamic necessity, Int. J. Numer. Meth. Heat & Fluid Flow. 17 (3) (2007) 322–332.
[52] D.A. Nield, The modeling of viscous dissipation in a saturated porous medium, ASME J. Heat Transf. 129 (2007) 1459–1463.
[53] T. Pesso, S. Piva, Laminar natural convection in a square cavity: low Prandtl numbers and large density differences, Int. J. Heat Mass Transf. 52 (2009) 1036–1043.
[54] J.M. Lopez, F. Marques, M. Avila, The Boussinesq approximation in rapidly rotating flows, J. Fluid Mech. 737 (2013) 56–77.
[55] P. Mayeli, G. Sheard, A new formulation for Boussinesq-type natural convection flows applied to the annulus cavity problem, Int. J. Numer. Methods Fluids 93 (3) (2021) 683–702.
[56] P. Mayeli, G. Sheard, Natural convection and entropy generation in square and skew cavities due to large temperature differences: A Gay-Lussac-type vorticity stream-function approach, Int. J. Numer. Methods Fluids (2021), https://doi.org/10.1002/fld.4980.
[57] B. Gebhart, J.C. Mollendorf, A new density relation for pure and saline water, Deep-Sea Res. 24 (1977) 831–848.
[58] M.W. Nansteel, K. Medjani, D.S. Lin, Natural convection of water near its density maximum in a rectangular enclosure: low Rayleigh number calculations, Phys. Fluids 30 (1987) 312–317.
[59] S.L. Braga, R. Viskanta, Transient natural convection of water near its density extremum in a rectangular cavity, Int. J. Heat Mass Transf. 35 (4) (1992) 861–875.
[60] A. Osorio, R. Avila, J. Cervantes, On the natural convection of water near its density inversion in an inclined square cavity, Int. J. Heat Mass Transf. 47 (19–20) (2004) 4491–4495.
[61] P. Vasseur, L. Robillard, B. Chandra Shekar, Natural convection heat transfer of water within a horizontal cylindrical annulus with density inversion effects, ASME: *J. Heat Transf.* 105 (1) (1983) 117–123.
[62] C.V. Raghavarao, Y.V.S.S. Sanyasiraju, Natural convection heat transfer of cold water between concentric cylinders, For high Rayleigh numbers – a numerical study, Int. J. Eng. Sci. **32** (1994) 1437–1450.
[63] C.J. Ho, Y.H. Lin, Natural convection heat transfer of cold water within an eccentric horizontal cylindrical annulus, ASME: J. Heat Transf. 110 (1988) 894–900.
[64] P. Wang, R. Kahawita, D.L. Nguyen, Transient natural convection with density inversion from a horizontal cylinder, Phys. Fluids A 4 (1992) 71–85.
[65] C.H. Lee, J.M. Hyun, H.S. Kwak, Oscillatory enclosed buoyant convection of a fluid with the density maximum, Int. J. Heat Mass Transf. 43 (19) (2000) 3747–3751.
[66] Z.Y. Zhong, K.T. Yang, J.R. Lioyd, Variable property effects in laminar natural convection in a square enclosure, ASME: J. Heat Transf. 107 (1985) 133–138.
[67] M.A. Leal, H.A. Machado, R.M. Cotta, Integral transform solutions of transient natural convection in enclosures with variable fluid properties, Int. J. Heat Mass Transf. 43 (2000) 3977–3990.
[68] J. Hernández, B. Zamora, Effects of variable properties and non-uniform heating on natural convection flows in vertical channels, Int. J. Heat Mass Transf. 48 (3–4) (2005) 793–807.
[69] D.N. Mahony, R. Kumar, E.H. Bishop, Numerical investigation of variable property effects on laminar natural convection of gases between two horizontal isothermal concentric cylinders, ASME: J. Heat Transf. 108 (4) (1986) 783–789.
[70] F. Shahraki, Modeling of buoyancy-driven flow and heat transfer for air in a horizontal annulus: effects of vertical eccentricity and temperature-dependent properties, Numer. Heat Transf. Part A 42 (6) (2002) 603–621.